The stressed brain - discovering the neural pathways to risk and resilience

Werff, S.J.A. van der

Author: Werff, S.J.A. van der
Title: The stressed brain - discovering the neural pathways to risk and resilience
Issue Date: 2017-01-10

Chapter 8

Structural and functional brain correlates of resilience to traumatic stress in Dutch police officers.

Discovering resilience in the brain

Steven J.A. van der Werff, Bernet M. Elzinga,
Annika Smit, Nic J.A. van der Wee

In Preparation

Abstract

Background

Neurobiological research has traditionally focused on vulnerability rather than on resilience to severe stress. So far, only a few neuroimaging studies examining resilience have used designs that allow disentangling of the neural correlates of resilience from those related to psychopathology or trauma-exposure alone. The aim of the present study was to identify structural brain correlates of resilience, their specific functional resting-state connectivity patterns and correlations with behavioral measures.

Methods

Multimodal MRI scanning was performed in three groups of police officers: (1) a resilient group (N = 29; trauma-exposed, no psychopathology), (2) a vulnerable group (N = 33; trauma-exposed, psychopathology), and (3) a control group (N = 19; no trauma, no psychopathology). Using whole brain and region-of-interest approaches, we examined gray matter volume, volume and shape of the hippocampus, white matter integrity, and resting-state functional connectivity using software tools from the FSL-library.

Results

In resilient police officers we found an increase in structural connectivity in a part of the corticopontine tract. We did not find specific patterns for gray matter volumes or volume and shape of the hippocampus. Areas directly adjacent to the structural connectivity results showed increased resting-state functional connectivity with the precuneus/posterior cingulate cortex region. Both structural and functional connectivity results correlated with scores for specific emotion regulation strategies.

Conclusions

Resilient police officers show a specific pattern of increased structural and functional connectivity that implies regions involved in self-processing and is correlated with the use of higher order emotion regulation strategies.

Introduction

By virtue of their profession, police officers have a higher chance of experiencing traumatic events compared to the general population. Stringent selection criteria for admission to police academies, including an extensive psychological assessment, exist to safeguard an elevated level of resilience in police officers. Moreover, training methods have been applied to further increase resilience to stress in police forces. Although in some cases experiencing traumatic events may lead to the development of trauma-related disorders like posttraumatic stress disorder (PTSD), major depressive disorders and anxiety disorders (Carlier et al., 1997; Berg et al., 2006; Maguen et al., 2009), there is no evidence that police officers suffer from more psychiatric symptomatology compared to individuals without high-risk occupations (van der Velden et al., 2013). This makes the police force an interesting group to study in light of resilience.

There has been a long and extensive research history into intrapsychological and intersocial mechanisms influencing resilience. Mechanisms involved in resilience include emotion regulation, coping styles, social support, self-efficacy, self-esteem, personality characteristics (e.g. optimism and extraversion), and mindfulness (Southwick et al., 2013). However, despite progress in neuroscience methods, research into the neurobiology of resilience to traumatic stress is still very limited. Information we do have is often based on studies that examine PTSD patients compared to trauma-exposed non-PTSD individuals (for a review see: (van der Werff et al., 2013). With this comparison, however, it remains unclear whether differences found between these two groups are to be attributed to trauma-related symptomatology in the patient group, or to the resilience in the control group. To be able to identify alterations in brain networks associated with resilience, a third group of individuals without traumatic experiences and without psychopathologies should be added to the design. As only a comparison of these three groups can elucidate the specific characteristics of the resilient individuals compared to the other two groups and thus which of the effects are specifically associated with resilience. Structural neuroimaging studies using magnetic resonance imaging (MRI) to study gray matter in trauma-exposed twins and non-trauma-exposed co-twins suggest that an increased size of the hippocampus is related to resilience (Gilbertson et al., 2002; Kasai et al., 2008). This is plausible considering the role of the hippocampus in memory consolidation and the important role of memory in trauma-related psychopathology (i.e., intrusive memories of traumatic experiences). The hippocampus is also important for stress regulation and contains high levels of mineralocorticoid receptors making it highly sensitive to glucocorticoids, which are released during the stress response. A reduction of hippocampal volume is often seen in stress-related psychiatric disorder (Gurvits et al., 1996; Bremner et al., 2003; Campbell et al., 2004; Kitayama et al., 2005; O'Doherty et al., 2015) and as a result of hypercortisolism (Starkman et al., 1992; Starkman et al., 1999).

The role of white matter structural connectivity has not yet been studied in the context of resilience. In stress-related disorders, decreases of white matter integrity of the uncinate fasciculus (Eluvathingal et al., 2006; Cullen et al., 2010) and the cingulum bundle (Fani et al., 2012; Daniels et al., 2013) have often been found, using diffusion tensor imaging (DTI). The uncinate fasciculus connects parts of the limbic system with the medial prefrontal cortex (mPFC). The mPFC inhibits fear responses and emotional responsiveness mediated by the amygdala (Sotres-Bayon et al., 2004), a process that has been found to be disturbed in stress-related psychiatric disorders, including PTSD (Elzinga and Bremner, 2002).

The cingulum bundle connects the hippocampus and the anterior cingulate cortex. The integrity of this tract directly influences the communication between the hippocampus and the anterior cingulate cortex, two regions that show altered function in PTSD (Elzinga and Bremner, 2002; Thomaes et al., 2013). However, it remains unclear whether these decreases in white matter integrity are purely associated the PTSD symptomatology or whether an increase of white matter integrity might also be indicative of resilience.

As to the best of our knowledge no study yet has examined the gray matter volume and white matter integrity correlates of resilience to traumatic stress in a design with a resilient group, a vulnerable group and a healthy control group.
We examined gray matter volume and white matter integrity to identify specific correlates of resilience in a cohort of Dutch police officers. Based on the existing literature we hypothesized to find an increase in gray matter volume of the hippocampus in trauma-exposed police officers without a history of psychopathology (the resilient group) compared to both trauma-exposed police officers with a history of psychopathology (the vulnerable group) and trauma non-exposed recruits from the police academy without a history of psychopathology (the control group). We also hypothesized to find an increase in white matter integrity of the uncinate fasciculus and the cingulum, specific for resilient officers. In addition to these region-of-interest (ROI) analyses, we performed an explorative whole brain analysis to detect structural correlates of resilience outside these a priori defined ROI's. In

addition, we explored associations between measures of structural connectivity and measures of functional connectivity as assessed with resting-state fMRI (RS-fMRI). For a better understanding of the results, we will associate these connectivity measures with resilience-related behavioral measurements.

Materials and Methods

Subjects

Trauma-exposed executive personnel of the Dutch police were recruited through advertisements on the intranet of the Dutch police force. For optimal homogeneity across groups the non-exposed healthy control group, was recruited from the Dutch police academy. A total of 149 subjects signed up and were screened for eligibility. Exclusion criteria for all subjects were: MRI contraindications such as metal implants, heart arrhythmia, claustrophobia and possible pregnancy, a history of neurological or other medical illness with central nervous system sequelae, the use of psychotropic medications other than stable use of SSRI's or infrequent benzodiazepine use (i.e., equivalent to 2 doses of 10 mg of oxazepam 3 times per week as a maximum and refrain from use 48 hours before scanning), a history of childhood maltreatment (i.e. < 18 years), a history of psychopathology with onset before work related traumatic events, left-handedness, insufficient knowledge of the Dutch language, and smoking > 5 cigarettes a day on average. 86 subjects were invited to participate in the study. Five subjects were excluded from the study after quality checking the MRI data, due to imaging artifacts in their respective MRI scans. The resulting 81 subjects were divided into three groups based on clinical assessment. The resilient group (N = 29) consists of individuals who report having experienced traumatic events, and do not fulfill the criteria for any DSM-IV diagnoses, either current or past. The vulnerable group (N = 33) consists of individuals who report having experienced traumatic events and fulfill the criteria for one or more DSM-IV diagnoses, either current or past. Individuals in this group met the criteria for the following diagnoses at least once in their lives, after graduating from the Police Academy: major depressive disorder (n = 27), panic disorder (n = 3), agoraphobia (n = 7), specific phobia (n = 1), social phobia (n = 2), generalized anxiety disorder (n = 2), posttraumatic stress disorder (n = 14), substance abuse (n = 8). The control group (N =19) consists of trainees recruited from the police academy who report no exposure to traumatic experiences and do not meet the criteria for any DSM-IV diagnosis in the present or past. Written informed consent was obtained from all participants before the clinical assessment and the MRI scan session. The medical ethical committee of the Leiden University Medical Center approved the study protocol. This study was designed and conducted in accordance with the principles of the declaration of Helsinki.

Behavioral Assessment

Past and current DSM-IV axis-1 psychiatric disorders were assessed using the mini-international neuropsychiatric interview (MINI)(van Vliet and de Beurs, 2007).
Severity of depressive symptoms were evaluated using the Montgomery-Asberg Depression Rating Scale (MADRS) (Montgomery and Asberg, 1979), and the Inventory of Depression Symptomatology (IDS) (Rush et al., 1996). Severity of anxiety symptoms was assessed using Becks Anxiety Inventory (BAI) (Beck et al., 1988). The Harvard Trauma Questionnaire (HTQ) was used to inquire trauma-related symptom severity (Mollica et al., 1992). The Connor-Davidson Resilience Scale (CD-RISC) was used to assess self-report resilience (Connor and Davidson, 2003). The Police Life Events Schedule (PLES) was used to assess the amount of exposure to work-related life events (Carlier et al., 1997). The Cognitive Emotion Regulation Questionnaire (CERQ) was used to assess cognitive coping strategies. This questionnaire consists of nine subscales which all measure a different coping strategy (Garnefski et al., 2001).

MRI Data Acquisition

Images were acquired on a Philips 3T MRI system (Philips Healthcare, Best, The Netherlands; software version 3.2.1). A SENSE-32 channel head coil was used for radio frequency transmission and reception.

For each subject four different scans were acquired including a high resolution anatomical scan, which was obtained using a sagittal three-dimensional gradient-echo T1-weighted sequence (repetition time=9.8 ms, echo time=4.6 ms, matrix size 256x256, voxel size 1.17x1.17x1.2 mm, 140 slices, scan duration 4:56 min).
DTI scans were acquired using a single-shot echo-planar imaging sequence with the following scan parameters: repetition time = 6250 ms, echo time = 70 ms, flip angle = 90°, b-factor = 1000 s/mm2, voxel dimensions = 2.07 x 2.12 x 2.10 mm, number of slices = 60, and no slice gap. DTI data were acquired along 32 directions, together with a baseline image having no diffusion weighting (b = 0). Total DTI scanning time was ~8 min.

RS-fMRI scans were acquired using T2*-weighted gradient-echo echo-planar imaging with the following scan parameters: 200 whole-brain volumes; repetition time (TR) = 2200 ms, echo time (TE) = 30 ms, flip angle = 80°, 38 slices, matrix size =

80 x 80, voxel size = 2.75 x 2.75 x 2.75 mm, scan duration = 7:28 min). Beforehand, the participants were instructed to lie as still as possible, with their eyes closed and without falling asleep. After completion of the scan all participants confirmed not having fallen asleep.

A high-resolution T2*-weighted gradient-echo echo-planar imaging scan (TR = 2200 ms, TE = 30 ms, flip angle = 80°, 84 axial slices, matrix size = 112 x112, voxel size =1.96 x 1.96 x 2 mm, no slice gap, scan duration = 46.2 s) was acquired for registration of the functional data to standard space.
A neuroradiologist, blinded for the clinical details of the subjects, examined all high resolution anatomical scans. No macroscopic abnormalities were observed.
All MRI data were processed using FSL (FMRIB's Software Library, www.fmrib.ox.ac.uk/fsl; (Smith et al., 2004) version 5.0.6).

Diffusion tensor imaging preprocessing
DTI data were corrected for distortion and motion artifacts induced by eddy currents or by simple head motions, using affine registration of each diffusion weighted image to the b = 0 reference image. Non-brain tissue was removed using the Brain Extraction Tool. Following, in order to generate individual fractional anisotropy (FA) maps for each participant, the diffusion tensor model was fitted to each voxel using FMRIB's diffusion toolbox (FDT). Tract-based spatial statistics (TBSS) version 1.2 was used for voxelwise analysis of the preprocessed FA data. First, individual FA images were aligned to the FMRIB58_FA standard-space image using nonlinear registration. Next, the mean FA image was generated and thinned to create a mean FA skeleton, which represents the centers of all tracts common to the entire group. The mean FA skeleton was then thresholded at a FA value of ≥0.45 to exclude peripheral tracts and minimize partial voluming. Finally, each participant's aligned FA images were projected onto the mean FA skeleton, and the resulting data were fed into voxelwise permutation-based analysis.

Resting-state fMRI preprocessing
Motion correction was applied to the RS-fMRI data along with non-brain tissue removal, spatial smoothing using a 6-mm full-width at half maximum (FWHM) Gaussian kernel, grand-mean intensity normalization of the entire 4D dataset by a single multiplicative factor and high-pass temporal filtering (Gaussian-weighted least-squares straight line fitting, 0.01 Hz cut-off). The RS-fMRI data of each participant were then registered to their respective high-resolution EPI images. The high-resolution EPI image was registered to the T1-weighted image,

and the T1-weighted image to MNI-152 standard space image. Resting-state data were analyzed using seed-based correlations. The seed was chosen immediately adjacent to the results of the DTI analysis. FSL-FIRST was used to segment this seed for each participant individually. These individual masks were then transformed to functional native space using the inverse transformation matrices obtained during registration in the preprocessing phase. Spatially averaged time series were extracted for each subject. A time series was also extracted for the global signal, white matter and cerebrospinal fluid. The timecourses that were extracted from the individual registered left putamen seeds were added as a regressor in a GLM. Nine nuisance regressors were included in the model: signal from the white matter, CSF signal, and the global signal, as well as six motion parameters (three translations and three rotations). The global signal was included to reduce artifacts associated with physiological signal sources (i.e. cardiac and respiratory; (Raichle et al., 2001; Birn et al., 2006). After reslicing the resulting individual correlation maps and their corresponding within-subject variance maps into 2 mm isotropic MNI space, they were entered into a higher level within and between groups mixed effects analysis (one- and two-sample t-test).

Gray Matter analyses

Details on MRI data acquisition, MRI preprocessing and behavioral measurements are reported in the supplementary materials.

All MRI analyses were conducted in FSL (FMRIB's Software Library, www.fmrib.ox.ac.uk/fsl; (Smith et al., 2004) version 5.0.6). To test our hypothesis that size of the hippocampus is different in resilient individuals we used FSL's Integrated Registration and Segmentation Tool (FIRST) to automatically segment both the left and right hippocampus and construct them as vertexes, which also allows comparisons of shape. This method searches through linear combinations of shape modes of variation for the most probable shape instance given the observed intensities in the T1-weighted image, based on learned models constructed from 336 subjects (Patenaude et al., 2011). To test whether there were any between-groups differences in shape of the hippocampus a 1x3 ANOVA design was modeled in the general linear model (GLM), with age and gender included as confound regressors, and tested using FSL's Randomise Tool, permutation-based (5000 permutations) non-parametric testing, correcting for multiple comparisons across space. Threshold free cluster enhancement (TFCE) was used for finding clusters in the data and threshold for significance was set on $p < 0.05$ TFCE corrected.

The explorative whole brain analysis was performed using a voxel-based morphometry approach (VBM) implemented in FSL. First, structural images were brain extracted and gray matter-segmented (Zhang et al., 2001). The resulting gray matter partial volume images were then aligned to MNI-152 (T1 standard brain average over 152 subjects; Montreal Neurological Institute, Montreal, QC, Canada) standard space, using affine registration, followed by nonlinear registration (Jenkinson et al., 2002). The resulting images of all participants were averaged to create a study-specific template, to which the native gray matter images were then nonlinearly reregistered. In order to correct for local expansion or contraction, the registered partial volume images were then modulated by dividing them by the Jacobian of the warp field. The modulated segmented images were then smoothed with an isotropic Gaussian kernel with a sigma of 3 mm. The Gaussian outputs a weighted average of each voxel's neighborhood, with the average weighted more toward the value of the centrally located voxels. The application of this type of smoothing reduces the noise in the data substantially. Finally, groups were compared using a GLM including age and gender as confound regressors. To investigate where the resilient group differentiated from both the vulnerable group and the control group the voxel-wise GLM tested an inversed quadratic model, using permutation-based (5000 permutations) non-parametric testing, correcting for multiple comparisons across space. TFCE was used for finding clusters in the data, with thresholds for both the ROI comparison as well as the whole brain analysis set on $p < 0.05$ corrected.

Diffusion tensor imaging analyses

To test for regional specific fractional anisotropy (FA) alterations, we first implemented a ROI-based tract-based spatial statistics (TBSS). A binary mask encompassing the bilateral uncinate fasciculus and the cingulum was created as a ROI using the Johns Hopkins University White Matter Atlas provided by FSL, with probability set to 15%-100%. The mask was then applied to the mean FA skeleton in order to include only voxels comprised in the mean FA skeleton. This confines the statistical analysis exclusively to voxels from the center of the tract, thereby minimizing anatomic inter-subject variability, registration errors, and partial voluming. The resulting study-specific ROI mask was used for voxelwise permutation-based ROI analysis.

Using FSL's Randomise Tool, permutation-based inferences with TFCE were carried out for voxelwise analysis of FA data. In both the ROI analysis and the whole brain analysis 5000 random permutations were generated to build up the null distribution of the cluster size statistic, while testing an inversed quadratic model to investigate where the resilient group differentiated from both the vulnerable group and the control group. Age and gender were included in the analysis as confound regressors to correct for between group variances. The resulting statistical maps were corrected for multiple comparisons ($p < 0.05$, TFCE corrected).

Post-Hoc Analyses

To enable further interpretation of the TBSS results a mask was created of the voxels that were found to differ significantly between groups on FA. Along with this mask, information on each individual's axial diffusivity (the 1st eigenvalue), radial diffusivity (the average of the 2nd and 3rd eigenvalues), and mean diffusivity was fed into FSL's Randomise Tool using permutation-based inferences with TFCE.

RS-fMRI scans were used to examine whether structural connectivity specific to resilient subjects was accompanied by differences in resting-state functional connectivity (RSFC) seeded from areas adjacent to the structural connectivity results. The seed was chosen based on the results of the DTI analysis. FSL-FIRST was used to segment this seed for each participant individually.

Individual correlation maps and their corresponding within-subject variance maps were entered into a higher level within and between groups mixed effects analysis (one- and two-sample t-test). For each subject, gray matter density maps were derived from the anatomical scans. To correct for the effects of possible misregistration (Oakes et al., 2007), information about gray matter density of each subject was included as a voxelwise confound regressor. To investigate where the resilient group differentiated from both the vulnerable group and the control group GLM tested an inversed quadratic model including age and gender as confound regressors. Cluster correction was applied with an initial cluster forming threshold of $Z > 2.3$ and a corrected $p < .05$.

To assess whether any of the effects are associated with specific emotion regulation styles within the resilient group, correlation analyses were performed using the FA values for structural connectivity, the Z-scores for the RSFC, and the scores on the CD-RISC and the nine subscales of the CERQ. Correlation analyses were performed using Pearson's r or, when data violated assumptions for parametric tests, with Kendall's tau.

Table 1. Demographics and Psychometric data

	Resilient		Vulnerable		Controls			
	N		**N**		**N**		***p* 1 vs 2**	***p* 1 vs 3**
N	29		33		19			
Females/Males	10/19		8/25		11/8		.413 [a]	.143 [a]
	Mean	**SD**	**Mean**	**SD**	**Mean**	**SD**	***p* 1 vs 2**	***p* 1 vs 3**
Age	40.24	11.84	44.24	11.19	25.16	4.63	.178 [b]	**<.001** [b]
IDS	36.10	6.97	43.67	12.55	33.37	5.70	**.008** [b]	.091 [b]
BAI	24.07	2.82	26.18	6.5	24.06	2.92	.246 [b]	.965 [b]
MADRS	1.72	2.36	5.21	7.53	.21	.713	.195 [b]	**.001** [b]
CD-RISC	98.96	12.06	92.09	14.24	102.63	9.75	**.05** [c]	.261 [c]
HTQ	34.72	5.13	43.67	14.67	33.95	5.45	**.008** [b]	.619 [b]
PLES (before outlier omission)	168.39	140.25	334.28	619.52	25.95	53.94	.534 [b]	**<.001** [b]
PLES (after outlier omission)	168.39	140.25	235.77	257.20	25.95	53.94	.671 [b]	**<.001** [b]
CERQ: Self-blame	7.65	2.74	8.52	3.29	8.16	2.32	.308 [b]	.394 [b]
CERQ: Blaming others	5.79	1.82	7.24	2.59	5.53	1.68	**.024** [b]	.703 [b]
CERQ: Acceptance	10.38	2.93	12.30	3.19	12.80	3.34	**.017** [b]	**.018** [b]
CERQ: Refocus on planning	13.69	3.71	13.81	3.18	14.47	2.80	.898 [b]	.503 [b]
CERQ: Positive refocusing	11.66	4.29	11.33	3.36	12.11	3.51	.742 [c]	.705 [c]
CERQ: Rumination	9.93	3.91	11.94	6.75	9.31	3.38	.150 [b]	.626 [b]
CERQ: Positive reappraisal	14.59	3.49	14.00	3.86	15.37	3.44	.723 [b]	.433 [b]
CERQ: Putting into perspective	11.66	4.15	11.30	3.37	13.16	3.53	.714 [c]	.201 [c]
CERQ: Catastrophizing	4.76	1.33	6.45	3.03	4.84	1.21	**.001** [b]	.767 [b]

[a] = Chi-Square test; [b] = Mann-Whitney U test; [c] = Independent Sample T-test. IDS = Inventory of depression symptomatology; BAI = Becks Anxiety Inventory; CD-RISC = Connor-Davidson Resilience Scale; HTQ = Harvard Trauma Questionnaire; MADRS = Montgomery-Asberg Depression Rating Scale; PLES = Police Life Events Schedule; CERQ = Cognitive Emotion Regulation Questionnaire. In bold are all p-values considered significant ($p < .05$).

Results

Psychometric data

Demographic and psychometric data are reported in Table 1. As expected, there was an age difference between the resilient group and the control group ($p < .001$), but not between the resilient group and the vulnerable group ($p = .178$). Furthermore, the resilient group reported higher scores on the CD-RISC compared to the vulnerable group ($p = 0.05$), but not compared to the control group ($p = .261$).

Scores on the PLES indicated that the resilient group experienced more work related life events compared to the control group ($p < .001$), but not compared to the vulnerable group ($p = .534$) validating our selection procedures. One outlier was present in the vulnerable group, reporting 3388 work-related life events. As a member of a vice squad, the subject reported over 3000 cases of exposure to adult sexual abuse; roughly one experience every day for the last 10 years. After omission of this outlier, mean scores of the resilient group and the vulnerable group on number of experienced work-related life events grew even closer ($p = .671$). The vulnerable group reported more trauma-related symptoms on the HTQ compared to the resilient group ($p = .008$), as well as higher depression scores on the IDS ($p = .008$). The average MADRS score for all the groups was below the norm for residual depressive symptoms (MADRS score < 6), with significantly lower scores in the resilient group compared to the vulnerable group ($p < 0.01$).

With respect to cognitive emotion regulation strategies measured using the CERQ, we found that the resilient group scored lower on the subscale acceptance compared to both the vulnerable group (p.017) and the control group ($p = .018$). In addition, the resilient group scored lower on blaming others ($p = .024$) and catastrophizing ($p = .001$) compared to the vulnerable group.

Gray Matter Structure Results

The shape analysis for both left ($p > 0.955$) and right ($p > 0.58$) hippocampus did not show significant differences in shape between groups. Information about individual volumes of the left and right hippocampus was extracted and subsequently analyzed using IBM SPSS statistics 20. A 1x3 ANCOVA test was used controlling for age and gender, both left ($p = .955$) and right ($p = .931$) hippocampus did not differ in volume between groups. The explorative whole brain VBM testing the inversed quadratic design did not show any significant results in gray matter volume with $p < 0.57$ for all voxels.

Tract-based spatial statistics

The ROI analysis of the FA values in the bilateral uncinate fasciculus and the cingulum bundle showed no significant inversed quadratic effect (for all voxels: $p > .77$, TFCE corrected). The explorative whole brain analyses, however, showed a significant inversed quadratic effect in FA values of the left corticopontine tract starting adjacent to the left putamen, leading up to cortical areas where it bends in the parietal direction ($p < .05$, TFCE corrected; Figure 1). Post-hoc analyses of the axial diffusivity, radial diffusivity, and mean diffusivity revealed that the effect in FA was driven by decreases of radial diffusivity and mean diffusivity (for both: $p < .001$) in the resilient group. The axial diffusivity values did not differ significantly between groups.

Figure 1. Structural connectivity specific for resilience

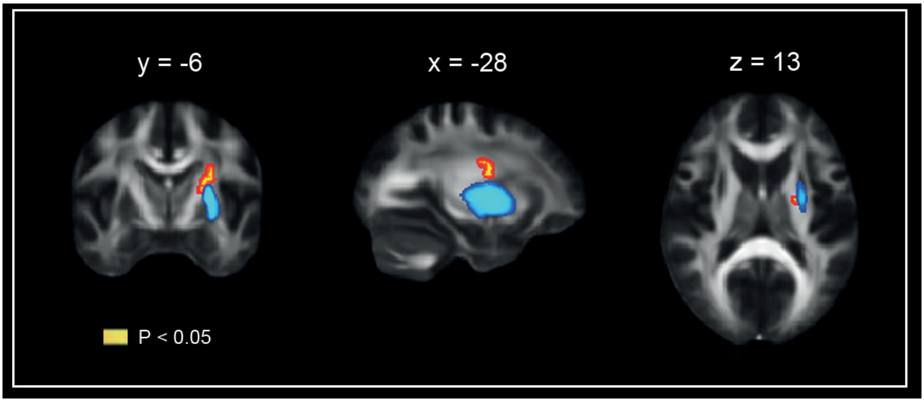

Coronal, sagittal and transversal slices of the FMRIB58_MNI_1mm standard brain (gray). Superimposed are the voxels that were found to have a significantly increased FA value in the resilient group (yellow; p <.05, TFCE corrected). For visibility reasons the tbss_fill command was used to thicken the effect (red). To further clarify the location of the effect, the left putamen is depicted (blue; Harvard-Oxford Subcortical Structural Atlas, probability: 30 -100 %). Images are in radiological convention (the right side of the image corresponds with the left hemisphere and vice versa).

Post-hoc resting-state functional connectivity analyses

Based on the location of the effect in white matter integrity, the seed of the RSFC was placed in the left putamen. Using FSL-FIRST, for each individual the left putamen was segmented and subsequently used as a seed in the RSFC analysis. We found increases in RSFC between the left putamen and an area containing the posterior cingulate cortex (PCC) and the precuneus, specific for resilient individuals (Figure 2a). Further investigation of the individual Z-scores indicating the strength of connectivity between the left putamen seed and the PCC/precuneus revealed that this effect was driven by an increase of negative connectivity in the resilient group compared to the other groups (Figure 2b).

Figure 2. Resting-state functional connectivity with the left putamen, specific for resilience

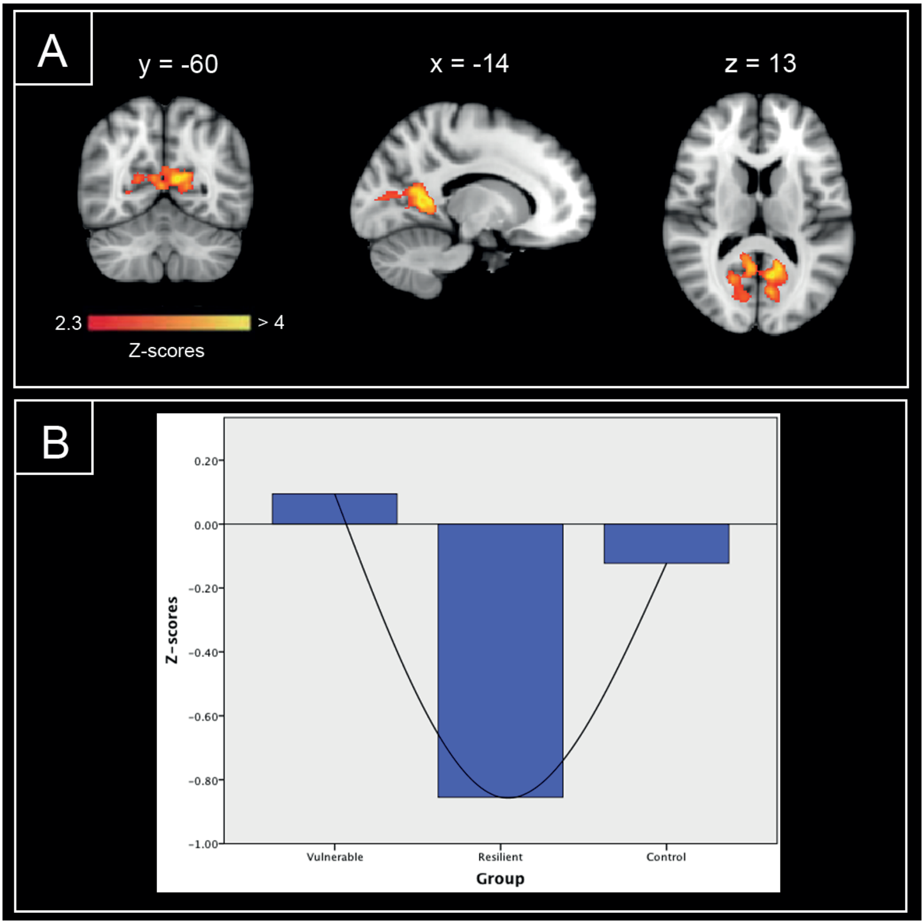

Coronal, sagittal and transversal slices of the MNI-152 1mm standard brain (gray). Superimposed is the region that was found significant in quadratic design of the study (red/yellow), indicating the pattern in resting-state functional connectivity with the left putamen specific for the resilient group. The effect resembles z-statistics with an initial cluster-forming threshold of z > 2.3 and p <.05, corrected. Images are in radiological convention (the right side of the images corresponds with the left hemisphere and vice versa (B). The mean z-score of the area that was tested significant depicted separately for each group. The line resembles the quadratic effect.

Post-hoc correlation analyses

To assess whether FA values in the area with significantly increased FA were related to self-report resilience or emotion regulation strategies within the resilient group, the mean FA values from this specific area were extracted and exported to SPSS.

The correlation coefficients of the FA values in the corticopontine tract with the CD-RISC scores and with the nine subscales of the CERQ were examined (Table 2). To correct for multiple comparisons we applied a Bonferroni correction and adjusted the level of significance to p <.005. We found a significant correlation between the positive reappraisal subscale of the CERQ and the FA values within the resilient group (p =.004). In addition, we found a significant correlation between the Z-scores reflecting the strength of the RSFC between the left putamen seed and the PCC/ precuneus and the positive reappraisal subscale of the CERQ (p =.037)

Table 2. Intercorrelations between structural connectivity and behavioral scales in resilient individuals

	FA		
Scales	**Pearson's r**	**Kendall's tau**	***p***
CD-RISC	.346		.066
CERQ: Self-blame	.000		1.00
CERQ: Blaming others		.058	.682
CERQ: Acceptance		.327	.018 *
CERQ: Refocus on planning	.426		.021 *
CERQ: Positive refocusing	.429		.020 *
CERQ: Rumination		.186	.168
CERQ: Positive reappraisal	.513		.004 **
CERQ: Putting into perspective	.145		.453
CERQ: Catastrophizing		.054	.716

FA = Fractional anisotropy; CD-RISC = Connor-Davidson Resilience Scale;
CERQ = Cognitive Emotion Regulation Questionnaire.
* = $p < .05$ (uncorrected); ** = $p < .005$ (bonferroni corrected)

8

Discussion

In this study we set out to investigate the gray matter structure and structural connectivity characteristics of resilience to traumatic stress in a sample of Dutch police officers. Considering that there is a clear lack of neurobiological studies focusing resilience, our hypotheses were based on previous studies on stress-related psychopathologies, such as PTSD. We hypothesized that resilient police officers would be characterized by increased volumes of the hippocampus, and an increase in white matter integrity of the uncinate fasciculus and cingulum bundle. We also performed additional explorative whole brain analyses on both volume and structural connectivity.

Using FSL-FIRST, we found no increases in volume of the hippocampus. In addition, the explorative whole brain analysis we performed using VBM showed no gray matter characteristics specific for resilience. Smaller hippocampi have been found to be associated with stress-related disorders (Gurvits et al., 1996; Bremner et al., 2003; Campbell et al., 2004), and as a result of hypercortisolism (Starkman et al., 1992; Starkman et al., 1999). However, there has been an ongoing debate on whether an increased size of the hippocampus could also be a marker of improved resilience. Our data in this particular cohort do not support such notion.

With respect to structural connectivity, we did not find increased white matter integrity of the uncinate fasciculus and cingulum in the resilient group, as we had hypothesized. However, our explorative whole brain analysis did indicate increases in white matter integrity of a part of the corticopontine tract starting adjacent to the left putamen, leading up to cortical areas where it bends in the parietal direction. The fact that these changes in white matter integrity were found in a new area that has not been reported in the PTSD literature suggests that resilience is not simply the opposite of having psychiatric symptoms, but rather an independent construct.

To be able to further interpret these findings in FA, we examined the axial diffusivity, radial diffusivity, and mean diffusivity values. We found that the increased FA in the resilient group was mostly driven by differences in radial diffusivity and mean diffusivity in the resilient group, and not by differences in axial diffusivity. This pattern of decreases in mean diffusivity and radial diffusivity is an indication for increaed myelination of the white matter tract in resilient individuals (Song et al., 2005; Alexander et al., 2007). Increased myelination promotes speed at which impulses travel along the myelinated tract, therefore increasing both structural and functional connectivity between areas connected by these fibers (Hartline, 2008). Previous tractography studies of the putamen confirmed that tracts originating from the putamen follow the corticopontine tract in dorsal direction to the cortex, where they connect to both frontal and parietal regions (Leh et al., 2007; Jarbo and Verstynen, 2015). To investigate whether the pattern of structural connectivity in the resilient group was accompanied by similar patterns in functional connectivity, we conducted a resting-state functional connectivity analysis using the left putamen as a seed. We found increases in RSFC between the left putamen and an area including the PCC and the precuneus specific for the resilient group. The finding of negative connectivity between these two areas is in line with previous research examining RSFC using a seed in the putamen (Di Martino et al., 2008). The precuneus /PCC region is an area involved in self-referential processing, self-consciousness, and autobiographic memory (Cavanna and Trimble, 2006; Cavanna, 2007). With respect to resilience it has already been shown that psychological constructs that influence resilience include self-efficacy and self-esteem, which suggests that activity and connectivity of the precuneus / PCC region could play an important role in resilience. Additionally, this area is an important constituent of the default mode network and aberrant functioning of the default mode network has been implicated in various psychiatric disorders including depression (Sambataro et al., 2013), anxiety (Zhao et al., 2007), and PTSD (Lanius et al., 2010). The putamen is, in addition to being involved in motor skills, also involved in learning and memory. More specifically, the putamen has an active role in the acquisition (learning) and storage (memory) of stimulus-response associations (Packard and Knowlton, 2002). The increases in both structural and functional connectivity between the precuneus/PCC region and the left putamen could indicate interplay between stimulus-response learning based on experiences (including severe stressful stimuli like traumatic events) and the image an individual has of oneself. Automatic negative self-cognitions are a symptom of stress-related disorders and increased connectivity between the putamen and the PCC / precuneus area might protect an individual from acquiring such symptoms as stimulus-response learning can be more effectively influenced by higher order self-images and processing. This notion is strengthened by the results of the correlation analyses. Within the resilient group we found a significant correlation between positive reappraisal and the FA values in our found effect. Moreover, we also found a negative correlation between the strength of the RSFC between the left putamen and the precuneus/PCC region and positive reappraisal within the resilient group. Of note, positive reappraisal did not differ between groups, whereas acceptance scores were lower in the resilient group compared to the other two groups. This could indicate a proactive attitude of resilient individuals, and a drive towards a willingness to change negative circumstances rather than accepting them.

There are some limitations to take into account. First, due to our cross-sectional design no causal conclusions can be drawn from the data. We cannot conclude whether the effects in structural and functional connectivity have always been present in the high resilient individuals, or were acquired under influence of severe stressful situations. Second, we did not find effects in the hypothesized ROI's, which were based on studies focusing on psychiatric symptomatology, but only in our whole brain analyses, giving this study an explorative nature.

To the best of our knowledge this is the first study specifically designed to investigate structural and connectivity characteristics of resilience, within a homogenous group of police officers. Future studies should include task-related fMRI paradigms, which could contribute to investigate changes in brain activity specific for resilience during the demands of externally presented tasks (i.e., during a stress reaction, or during emotion regulation). Furthermore, longitudinal designs should be implemented to enable investigation of the causal pathway of the neural correlates of resilience. We also recommend adding a non-exposed healthy control group from the general population to provide more variation, as the majority of the police officers is already high resilient compared to the general population due to selection and training.

References

Alexander, A.L., Lee, J.E., Lazar, M., and Field, A.S. (2007). Diffusion tensor imaging of the brain. *Neurotherapeutics: the journal of the American Society for Experimental NeuroTherapeutics* 4, 316-329.

Beck, A.T., Epstein, N., Brown, G., and Steer, R.A. (1988). An inventory for measuring clinical anxiety: psychometric properties. *Journal of consulting and clinical psychology* 56, 893-897.

Berg, A.M., Hem, E., Lau, B., and Ekeberg, O. (2006). An exploration of job stress and health in the Norwegian police service: a cross sectional study. *Journal of occupational medicine and toxicology* 1, 26.

Birn, R.M., Diamond, J.B., Smith, M.A., and Bandettini, P.A. (2006). Separating respiratory-variation-related fluctuations from neuronal-activity-related fluctuations in fMRI. *NeuroImage* 31, 1536-1548.

Bremner, J.D., Vythilingam, M., Vermetten, E., Southwick, S.M., Mcglashan, T., Nazeer, A., Khan, S., Vaccarino, L.V., Soufer, R., Garg, P.K., Ng, C.K., Staib, L.H., Duncan, J.S., and Charney, D.S. (2003). MRI and PET study of deficits in hippocampal structure and function in women with childhood sexual abuse and posttraumatic stress disorder. *The American journal of psychiatry* 160, 924-932.

Campbell, S., Marriott, M., Nahmias, C., and Macqueen, G.M. (2004). Lower hippocampal volume in patients suffering from depression: a meta-analysis. *The American journal of psychiatry* 161, 598-607.

Carlier, I.V., Lamberts, R.D., and Gersons, B.P. (1997). Risk factors for posttraumatic stress symptomatology in police officers: a prospective analysis. *The Journal of nervous and mental disease* 185, 498-506.

Cavanna, A.E. (2007). The precuneus and consciousness. *CNS spectrums* 12, 545-552.

Cavanna, A.E., and Trimble, M.R. (2006). The precuneus: a review of its functional anatomy and behavioural correlates. *Brain: a journal of neurology* 129, 564-583.

Connor, K.M., and Davidson, J.R. (2003). Development of a new resilience scale: the Connor-Davidson Resilience Scale (CD-RISC). *Depression and anxiet*y 18, 76-82.

Cullen, K.R., Klimes-Dougan, B., Muetzel, R., Mueller, B.A., Camchong, J., Houri, A., Kurma, S., and Lim, K.O. (2010). Altered white matter microstructure in adolescents with major depression: a preliminary study. *Journal of the American Academy of Child and Adolescent Psychiatry* 49, 173-183 e171.

Daniels, J.K., Lamke, J.P., Gaebler, M., Walter, H., and Scheel, M. (2013). White matter integrity and its relationship to PTSD and childhood trauma--a systematic review and meta-analysis. *Depression and anxiety* 30, 207-216.

Di Martino, A., Scheres, A., Margulies, D.S., Kelly, A.M., Uddin, L.Q., Shehzad, Z., Biswal, B., Walters, J.R., Castellanos, F.X., and Milham, M.P. (2008). Functional connectivity of human striatum: a resting state FMRI study. *Cerebral cortex* 18, 2735-2747.

Eluvathingal, T.J., Chugani, H.T., Behen, M.E., Juhasz, C., Muzik, O., Maqbool, M., Chugani, D.C., and Makki, M. (2006). Abnormal brain connectivity in children after early severe socioemotional deprivation: a diffusion tensor imaging study. *Pediatrics* 117, 2093-2100.

Elzinga, B.M., and Bremner, J.D. (2002). Are the neural substrates of memory the final common pathway in posttraumatic stress disorder (PTSD)? *Journal of affective disorders* 70, 1-17.

Fani, N., King, T.Z., Jovanovic, T., Glover, E.M., Bradley, B., Choi, K., Ely, T., Gutman, D.A., and Ressler, K.J. (2012). White matter integrity in highly traumatized adults with and without post-traumatic stress disorder. *Neuropsychopharmacology: official publication of the American College of Neuropsychopharmacology* 37, 2740-2746.

Garnefski, N., Kraaij, V., and Spinhoven, P. (2001). Negative life events, cognitive emotion regulation and emotional problems. *Personality and Individual differences* 30, 1311-1327.

Gilbertson, M.W., Shenton, M.E., Ciszewski, A., Kasai, K., Lasko, N.B., Orr, S.P., and Pitman, R.K. (2002). Smaller hippocampal volume predicts pathologic vulnerability to psychological trauma. *Nature neuroscience* 5, 1242-1247.

Gurvits, T.V., Shenton, M.E., Hokama, H., Ohta, H., Lasko, N.B., Gilbertson, M.W., Orr, S.P., Kikinis, R., Jolesz, F.A., Mccarley, R.W., and Pitman, R.K. (1996). Magnetic resonance imaging study of hippocampal volume in chronic, combat-related posttraumatic stress disorder. *Biological psychiatry* 40, 1091-1099.

Hartline, D.K. (2008). What is myelin? *Neuron glia biology* 4, 153-163.

Jarbo, K., and Verstynen, T.D. (2015). Converging structural and functional connectivity of orbitofrontal, dorsolateral prefrontal, and posterior parietal cortex in the human striatum. *The Journal of neuroscience: the official journal of the Society for Neuroscience* 35, 3865-3878.

Jenkinson, M., Bannister, P., Brady, M., and Smith, S. (2002). Improved optimization for the robust and accurate linear registration and motion correction of brain images. *NeuroImage* 17, 825-841.

Kasai, K., Yamasue, H., Gilbertson, M.W., Shenton, M.E., Rauch, S.L., and Pitman, R.K. (2008). Evidence for acquired pregenual anterior cingulate gray matter loss from a twin study of combat-related posttraumatic stress disorder. *Biological psychiatry* 63, 550-556.

Kitayama, N., Vaccarino, V., Kutner, M., Weiss, P., and Bremner, J.D. (2005). Magnetic resonance imaging (MRI) measurement of hippocampal volume in posttraumatic stress disorder: a meta-analysis. *Journal of affective disorder*s 88, 79-86.

Lanius, R.A., Bluhm, R.L., Coupland, N.J., Hegadoren, K.M., Rowe, B., Theberge, J., Neufeld, R.W., Williamson, P.C., and Brimson, M. (2010). Default mode network connectivity as a predictor of post-traumatic stress disorder symptom severity in acutely traumatized subjects. *Acta* *psychiatrica Scandinavica* 121, 33-40.

Leh, S.E., Ptito, A., Chakravarty, M.M., and Strafella, A.P. (2007). Fronto-striatal connections in the human brain: a probabilistic diffusion tractography study. *Neuroscience letters* 419, 113-118.

Maguen, S., Metzler, T.J., Mccaslin, S.E., Inslicht, S.S., Henn-Haase, C., Neylan, T.C., and Marmar, C.R. (2009). Routine work environment stress and PTSD symptoms in police officers. *The Journal of nervous and mental diseas*e 197, 754-760.

Mollica, R.F., Caspi-Yavin, Y., Bollini, P., Truong, T., Tor, S., and Lavelle, J. (1992). The Harvard Trauma Questionnaire. Validating a cross-cultural instrument for measuring torture, trauma, and posttraumatic stress disorder in Indochinese refugees. *The Journal of nervous and mental disease* 180, 111-116.

Montgomery, S.A., and Asberg, M. (1979). A new depression scale designed to be sensitive to change. The British journal of psychiatry: the journal of mental scienc*e 134, 382-389.*

O'doherty, D.C., Chitty, K.M., Saddiqui, S., Bennett, M.R., and Lagopoulos, J. (2015). A systematic review and meta-analysis of magnetic resonance imaging measurement of structural volumes in posttraumatic stress disorder. *Psychiatry research* 232, 1-33.

Oakes, T.R., Fox, A.S., Johnstone, T., Chung, M.K., Kalin, N., and Davidson, R.J. (2007). Integrating VBM into the General Linear Model with voxelwise anatomical covariates. *NeuroImage* 34, 500-508.

Packard, M.G., and Knowlton, B.J. (2002). Learning and memory functions of the Basal Ganglia. *Annual review of neuroscience* 25, 563-593.

Patenaude, B., Smith, S.M., Kennedy, D.N., and Jenkinson, M. (2011). A Bayesian model of shape and appearance for subcortical brain segmentation. *NeuroImage* 56, 907-922.

Raichle, M.E., Macleod, A.M., Snyder, A.Z., Powers, W.J., Gusnard, D.A., and Shulman, G.L. (2001). A default mode of brain function. *Proceedings of the National Academy of Sciences of the United States of America* 98, 676-682.

Rush, A.J., Gullion, C.M., Basco, M.R., Jarrett, R.B., and Trivedi, M.H. (1996). The Inventory of Depressive Symptomatology (IDS): psychometric properties. *Psychological medicine* 26, 477-486.

Sambataro, F., Wolf, N.D., Pennuto, M., Vasic, N., and Wolf, R.C. (2013). Revisiting default mode network function in major depression: evidence for disrupted subsystem connectivity. *Psychological medicine*, 1-11.

Smith, S.M., Jenkinson, M., Woolrich, M.W., Beckmann, C.F., Behrens, T.E., Johansen-Berg, H., Bannister, P.R., De Luca, M., Drobnjak, I., Flitney, D.E., Niazy, R.K., Saunders, J., Vickers, J., Zhang, Y., De Stefano, N., Brady, J.M., and Matthews, P.M. (2004). Advances in functional and structural MR image analysis and implementation as FSL. *NeuroImage* 23 Suppl 1, S208-219.

Song, S.K., Yoshino, J., Le, T.Q., Lin, S.J., Sun, S.W., Cross, A.H., and Armstrong, R.C. (2005).

Demyelination increases radial diffusivity in corpus callosum of mouse brain. *NeuroImage* 26, 132-140.

Sotres-Bayon, F., Bush, D.E., and Ledoux, J.E. (2004). Emotional perseveration: an update on prefrontal-amygdala interactions in fear extinction. L*earning & memory* 11, 525-535.

Southwick, S., Litz, B.T., Charney, D., and Friedman, M.J. (2013). *Resilience and mental Health: Challenges across the lifespan.* Cambridge: Cambridge University Press.

Starkman, M.N., Gebarski, S.S., Berent, S., and Schteingart, D.E. (1992). Hippocampal formation volume, memory dysfunction, and cortisol levels in patients with Cushing's syndrome. *Biol Psychiatry* 32, 756-765.

Starkman, M.N., Giordani, B., Gebarski, S.S., Berent, S., Schork, M.A., and Schteingart, D.E. (1999). Decrease in cortisol reverses human hippocampal atrophy following treatment of Cushing's disease. *Biol Psychiatry* 46, 1595-1602.

Thomaes, K., Dorrepaal, E., Draijer, N., De Ruiter, M.B., Elzinga, B.M., Sjoerds, Z., Van Balkom, A.J., Smit, J.H., and Veltman, D.J. (2013). Increased anterior cingulate cortex and hippocampus activation in Complex PTSD during encoding of negative words. *Social cognitive and affective neuroscience* 8, 190-200.

Van Der Velden, P.G., Rademaker, A.R., Vermetten, E., Portengen, M.A., Yzermans, J.C., and Grievink, L. (2013). Police officers: a high-risk group for the development of mental health disturbances? A cohort study. *BMJ open* 3.

Van Der Werff, S.J., Van Den Berg, S.M., Pannekoek, J.N., Elzinga, B.M., and Van Der Wee, N.J. (2013). Neuroimaging resilience to stress: a review. *Frontiers in behavioral neuroscience* 7, 39.

Van Vliet, I.M., and De Beurs, E. (2007). [The MINI-International Neuropsychiatric Interview. A brief structured diagnostic psychiatric interview for DSM-IV en ICD-10 psychiatric disorders]. *Tijdschrift voor psychiatrie* 49, 393-397.

Zhang, Y., Brady, M., and Smith, S. (2001). Segmentation of brain MR images through a hidden Markov random field model and the expectation-maximization algorithm. *IEEE transactions on medical imaging* 20, 45-57.

Zhao, X.H., Wang, P.J., Li, C.B., Hu, Z.H., Xi, Q., Wu, W.Y., and Tang, X.W. (2007). Altered default mode network activity in patient with anxiety disorders: an fMRI study. *European journal of radiology* 63, 373-378.